

# Rosuvastatin Blocks hERG Current and Prolongs Cardiac Repolarization

ISABELLE PLANTE,<sup>1,2</sup> PATRICK VIGNEAULT,<sup>3,4</sup> BENOÎT DROLET,<sup>3,4</sup> JACQUES TURGEON<sup>1,2</sup>

<sup>1</sup>CRCHUM, Research Center, Centre Hospitalier de l'Université de Montréal, Montreal, Quebec, Canada H2W 1T7

<sup>2</sup>Faculty of Pharmacy, Université de Montréal, Montreal, Quebec, Canada H3C 3J7

<sup>3</sup>Research Center, Institut universitaire de cardiologie et de pneumologie de Québec, Quebec City, Quebec, Canada G1V 4G5

<sup>4</sup>Faculty of Pharmacy, Université Laval, Quebec City, Quebec, Canada G1V 0A6

Received 23 June 2011; revised 20 September 2011; accepted 17 October 2011

Published online 11 November 2011 in Wiley Online Library (wileyonlinelibrary.com). DOI 10.1002/jps.22809

**ABSTRACT:** Blocking of the potassium current  $I_{Kr}$  [human ether-a-go-go related gene (*hERG*)] is generally associated with an increased risk of long QT syndrome (LQTS). The 3-hydroxy-3-methyl-glutaryl-coenzyme A reductase inhibitor, rosuvastatin, is a methanesulfonamide derivative, which shows structural similarities with several  $I_{Kr}$  blockers. Hence, we assessed the effects of rosuvastatin on cardiac repolarization by using *in vitro*, *ex vivo*, and *in vivo* models. Patch clamp experiments on hERG-transfected human embryonic kidney (HEK) 293 cells established the potency of rosuvastatin to block hERG [half maximal inhibitory concentration ( $IC_{50}$ ) = 195 nM]. We showed in isolated guinea pig hearts that 195 nM rosuvastatin prolonged (basic cycle length of 250 ms;  $p < 0.05$ ) the monophasic action potential duration at 90% repolarization ( $MAPD_{90}$ ) by  $11 \pm 1$  ms. Finally, rosuvastatin (10 mg/kg, intraperitoneal) prolonged corrected QT interval (QTc) in conscious and unrestrained guinea pigs from  $201 \pm 1$  to  $210 \pm 2$  ms ( $p < 0.05$ ). Thus, rosuvastatin blocks  $I_{Kr}$  and prolongs cardiac repolarization. In additional experiments, we also show that hERG blockade in HEK 293 cells was modulated by coexpression of efflux [breast cancer resistance protein (BCRP), multidrug resistance gene (MDR1)] and influx [organic anion transporting polypeptide (OATP) 2B1] transporters involved in the disposition and cardiac distribution of the drug. Genetic polymorphisms observed for BCRP, MDR1, and OATP2B1, and  $IC_{50}$  determined for hERG blocking lead us to propose that some patients may be at risk of rosuvastatin-induced LQTS. © 2011 Wiley Periodicals, Inc. and the American Pharmacists Association *J Pharm Sci* 101:868–878, 2012

**Keywords:** potassium current; cardiac repolarization; drugs; long QT syndrome; torsades de pointes

## INTRODUCTION

Delayed rectifier current ( $I_K$ ) is a major outward potassium current responsible for the termination of the action potential plateau phase in human ventricular myocytes.  $I_K$  includes both rapidly ( $I_{Kr}$ ) and slowly ( $I_{Ks}$ ) activating components.<sup>1</sup> The  $I_{Kr}$  component is encoded in human by the human ether-a-go-go related gene (*hERG*; *KCNH2*), whereas  $I_{Ks}$  is encoded by *KvLQT1* (*KCNQ1*) and *minK* (*KCNE1*), which coassemble to form a channel.<sup>2,3</sup> Structure–

activity relationship studies have shown that  $I_{Kr}$  is selectively blocked by methanesulfonamide class III antiarrhythmic agents such as E-4031, ibutilide, dofetilide, and sotalol, whereas  $I_{Ks}$  is blocked by drugs such as clofilium, propofol, and indapamide.<sup>4–10</sup>

At the end of the 1990s, some drugs were withdrawn from the market due to reports of sudden cardiac death (such as cisapride and terfenadine), whereas others were forced to carry warning labels and to be used as last resort therapies due to the risk of proarrhythmic events.<sup>11–13</sup> The causative factors are not completely identified at present. However, extensive block of  $I_{Kr}$ , which may be associated with the induction of serious ventricular arrhythmias (such as torsades de pointes), is often implicated.<sup>14</sup> Indeed, the occurrence of  $I_{Kr}$  block by a new

Correspondence to: Jacques Turgeon (Telephone: +514-890-8044; Fax: +514-412-7186; E-mail: jacques.turgeon.chum@sss.gouv.qc.ca)

*Journal of Pharmaceutical Sciences*, Vol. 101, 868–878 (2012)  
© 2011 Wiley Periodicals, Inc. and the American Pharmacists Association

investigational drug, especially when the block is observed in the range of therapeutic plasma concentrations, usually terminates the development of this drug. In this regard, our laboratory demonstrated that non-antiarrhythmic drugs such as cisapride, domperidone, and risperidone can cause inhibition of  $I_{Kr}$  at clinically relevant concentrations.<sup>15–17</sup> We also found it to be the case for several other drugs such as erythromycin, thioridazine, droperidol, diphenhydramine, sildenafil, and pimozone.<sup>18–23</sup>

Rosuvastatin is a 3-hydroxy-3-methyl-glutaryl-coenzyme A (HMG-CoA) reductase inhibitor, which is very effective in lowering low-density lipoprotein (LDL) cholesterol, triglycerides, and C-reactive protein levels.<sup>24</sup> The drug is not metabolized by the cytochrome (CY) P450 system, and its clearance is mostly mediated by influx and efflux transporters from the ATP-binding cassette family [breast cancer resistance protein (BCRP), *ABCG2*] or the organic anion transporter family [organic anion transporting polypeptide (OATP) 1B1 (*SLCO1B1*), OATP1B3 (*SLCO1B3*), and OATP2B1 (*SLCO2B1*)].<sup>25,26</sup> Large intersubject variability is observed in peak plasma levels, which vary from 10 to 100 ng/mL (21 to 208 nM) at 40-mg dose.<sup>27</sup> Drug–drug interactions and genetic polymorphisms modulating drug transporter activity are major determinants of rosuvastatin pharmacokinetics. For instance, plasma concentrations of rosuvastatin increased 10-fold during the coadministration of cyclosporine and almost fivefold during the combined administration of lopinavir–ritonavir due to the inhibition of transporter activities.<sup>28,29</sup> Significant increases were also observed during the coadministration of gemfibrozil.<sup>30</sup> Pharmacogenetic studies have also shown a doubling in the mean plasma concentrations of rosuvastatin in Caucasians homozygous (AA) for the *ABCG2* (BCRP) variant allele C421A or homozygous (CC) for the *SLCO1B1*\*5 variant (T521C) allele.<sup>27,31</sup>

We noticed that the chemical structure of rosuvastatin shows similarities with the structure of several  $I_{Kr}$  blockers, including the presence of a methanesulfonamide moiety (Fig. 1). This led us to propose that rosuvastatin may show affinity for  $I_{Kr}$  and prolong the QT interval. The objectives of our studies were: (1) to determine the extent of hERG blockade by rosuvastatin, (2) to determine the modulatory role of membrane transporters on the extent of hERG blockade by rosuvastatin, and (3) to demonstrate the rosuvastatin's effects on cardiac repolarization using *ex vivo* (Langendorff retroperfused, isolated guinea pig hearts) and *in vivo* models (measurement of the QT interval in conscious guinea pigs) validated for the assessment of drug effects on cardiac repolarization.

## METHODS

### Human Embryonic Kidney 293 Cell Preparation and Electrophysiological Measurements

*hERG*-stably transfected human embryonic kidney (HEK) 293 cells were kindly donated by Dr. Craig T. January (University of Wisconsin–Madison, Madison, Wisconsin). Cells were cultured, harvested, and transferred to a bath mounted on the stage of an inverted microscope, as described previously.<sup>20</sup> For membrane current recordings (baseline conditions), cells were superfused with HEPES-buffered Tyrode's solution containing (in mM) 137 NaCl, 4 KCl, 1.8 CaCl<sub>2</sub>, 1 MgCl<sub>2</sub>, 10 glucose, and 10 HEPES (pH 7.4 with NaOH). Cells were then superfused for 15 min (1 mL/min) with Tyrode's solutions containing five different concentrations of rosuvastatin acid form (19.6–979.2 nM). Membrane currents were recorded to measure the percentage of block of the hERG tail current induced by each rosuvastatin concentration. Finally, cells were superfused for 20 min with the baseline Tyrode's solution to observe the reversibility of drug effects on the hERG block (washout conditions). Membrane currents were recorded in whole-cell configuration using suction pipettes.<sup>20</sup> All experiments were performed at 30°C.

### Transfection Procedure

In order to evaluate the effects of different transporters on the block of hERG by rosuvastatin, the *hERG*-stably transfected HEK 293 cells were transiently transfected with 10 µg of a recombinant pIRES2 vector expressing the green fluorescent protein (GFP) and one or the other of the following transporters: efflux transporter BCRP (strong affinity for rosuvastatin), loss of function variants of BCRP (BCRP-F208S, BCRP-S441N, and BCRP-Q141K), the influx transporters OATP2B1 (strong affinity for rosuvastatin), and multidrug resistance gene (*MDR1*) (an efflux transporter showing weak affinity for rosuvastatin). The transfection was performed using the calcium phosphate precipitation technique. Briefly, 10 µg of the recombinant vector was mixed with 300 µL of CaCl<sub>2</sub> (250 mM) and then this solution was added dropwise to a 300 µL aliquot of 2× HEPES-buffered saline containing (in mM) 280 NaCl, 50 HEPES, and 1.5 NaH<sub>2</sub>PO<sub>4</sub> (pH adjusted to 7.05 with HCl). Only green fluorescent cells were selected and voltage clamped in the whole-cell configuration 48–72 h after transfection at 30°C.

### Site-Directed Mutagenesis

The three loss-of-function variants of BCRP (BCRP-F208S, BCRP-S441N, and BCRP-Q141K) were

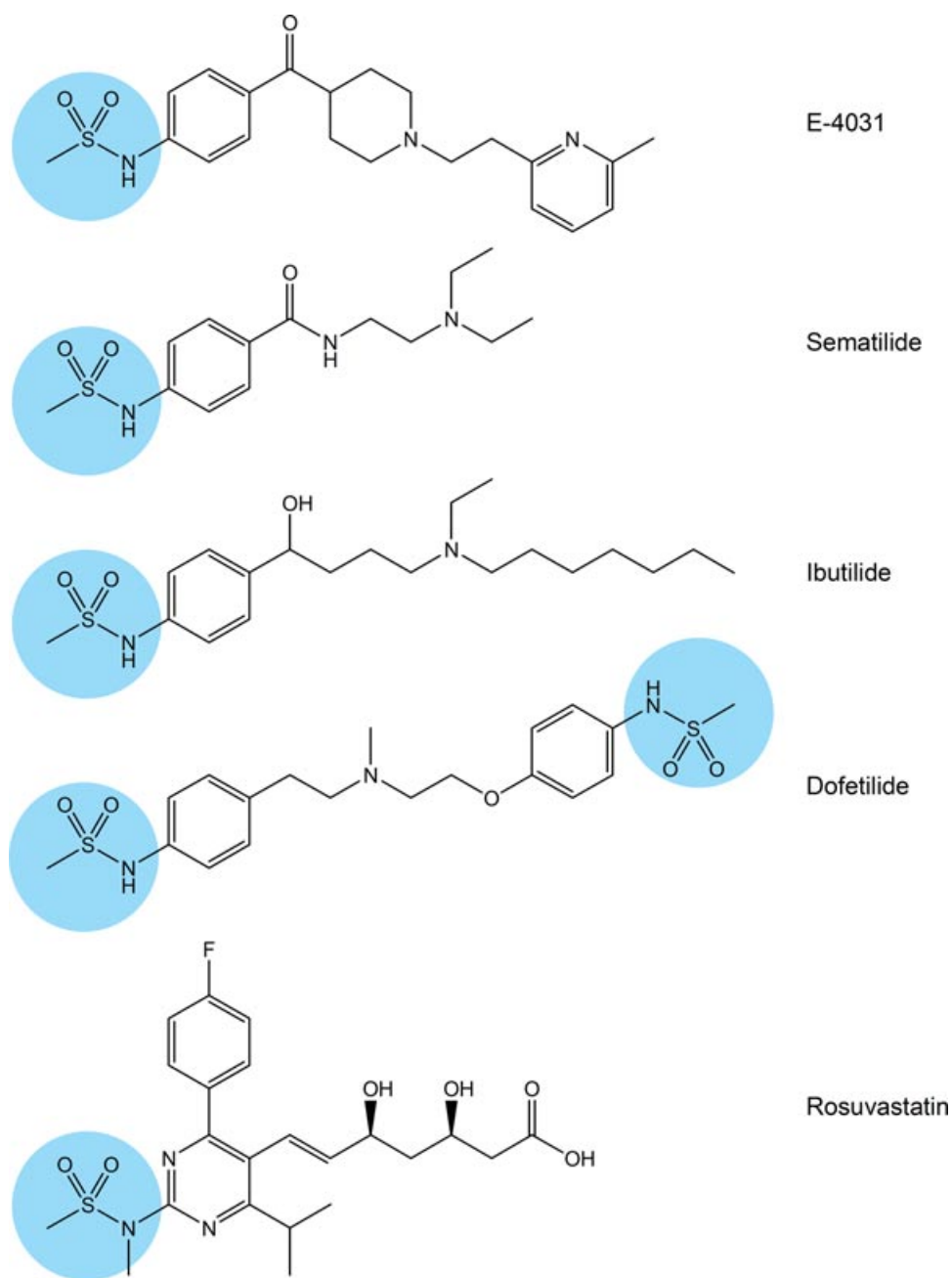


**Figure 1.** Chemical structures of rosuvastatin and methanesulfonamide derivatives associated with the block of hERG/ $I_{Kr}$ . Circles show methanesulfonamide moieties.

produced from the recombinant vector pIRES2BCRP-GFP using the QuikChange *site-directed mutagenesis kit* from Stratagene (La Jolla, California) according to the manufacturer's protocol (catalog #200519).

#### Drug Preparation

Rosuvastatin diacid calcium salt (Toronto Research Chemicals Inc., North York, Ontario, Canada) was dissolved in dimethyl sulfoxide (DMSO; Sigma-Aldrich, Inc., St. Louis, Missouri) and added to the HEPES-buffered Tyrode's solution to yield final concentrations of 19.6, 78.4, 156.8, 313.6, and

979.2 nM of rosuvastatin acid. For each concentration tested, an equivalent volume of DMSO was added to the HEPES-buffered Tyrode's solution used during the measurements recorded at baseline and washout. The maximal DMSO concentration (for 979.2 nM rosuvastatin) was 0.05% (v/v), a concentration known and previously shown not to interfere with hERG activity.<sup>15</sup>

#### Patch Clamp Protocol

Effects of rosuvastatin on the hERG current were studied in cells clamped at a holding potential

of  $-80$  mV. Depolarizing steps were applied for 4 s to voltages between  $-50$  and  $+50$  mV in 10-mV increments. Deactivating tail currents were measured at  $-40$  mV for 6 s before cells were returned to the holding potential ( $-80$  mV). Currents were low-pass filtered at 1 KHz (four-pole Bessel filter;  $-3$  dB/octave) and sampled at 2 KHz. Cells were exposed to one of the five rosuvastatin concentrations studied ( $n = 5-8$  cells per concentration) to determine the effects of rosuvastatin on hERG current. The amplitude of hERG tail current relative to the baseline was plotted against the log of rosuvastatin concentrations studied. Then, the data were fitted to the Hill's equation in order to estimate the half maximal inhibitory concentration ( $IC_{50}$ ) of rosuvastatin for block of hERG.

### Housing and Use of Animals

Experiments were performed in accordance with our institutional guidelines on animal use in research. Animals were housed and maintained in compliance with the Guide to the Care and Use of Experimental Animals of the Canadian Council on Animal Care.

### Langendorff Retroperfusion Experiments

Male Hartley guinea pigs ( $n = 11$ ; Charles River Laboratories, Montreal, Quebec, Canada) weighing 350–450 g were anticoagulated by intraperitoneal (i.p.) injection of heparin sodium (400 IU). Thirty minutes later, animals were killed by cervical dislocation and the hearts were rapidly extirpated and immersed in cold ( $4^{\circ}\text{C}$ ) Krebs–Henseleit buffer containing (in mmol/L) glucose 5, KCl 4.7,  $\text{CaCl}_2$  1.2,  $\text{NaHCO}_3$  25, NaCl 118.5,  $\text{MgSO}_4$  2.5, and  $\text{KH}_2\text{PO}_4$  1.2. This solution was continuously gassed with 95% oxygen and 5% carbon dioxide (pH 7.4,  $37^{\circ}\text{C}$ ). Each heart was cannulated and retrogradely perfused via the aorta with the buffer at a constant pressure equivalent to 70 mmHg using a custom-made isolated heart IH-SR double-warming coil heart perfusion system from Hugo Sachs Elektronik–Harvard Apparatus (March-Hugstetten, Germany). Hearts were electrically stimulated at a basic pacing cycle length (BCL) of 250 ms (4 Hz, approximately the natural sinus rate for guinea pigs and the slowest possible to work with when one wishes to avoid atrioventricular nodal ablation) with a small coaxial stimulation electrode connected to a programmable stimulator module. Monophasic action potential (MAP)-tip recording electrodes were securely positioned on the surface (epicardium) of each ventricle to obtain visually adequate signals (amplitude  $> 25$  mV, stable phase 4). Both MAP signals were continuously recorded (digital sampling rate 1 kHz), along with perfusion pressure, and stored on hard disk for analysis. These values were averaged by use of a routine designed specifically for this pur-

pose and incorporated in the analysis algorithm of the ISOHEART software package from Hugo Sachs Elektronik. At least 12 complexes were used for each measurement. MAP signals were recorded at a BCL of 250 ms. Then, to assess rate dependency, BCL was changed to 200 ms and the heart was paced for 1 min before the MAP was recorded. The same procedure was repeated for BCL of 150 ms. Thereafter, perfusion was performed with a buffer containing rosuvastatin 195 nM [dissolved in 50  $\mu\text{L}$  of DMSO; final DMSO in buffer 0.01% (v/v)] for a period of 15 min at a BCL of 250 ms. To assess the rate-dependent effects of the drug, MAP signals were recorded again at BCLs of 200 and 150 ms. Perfusion with a buffer containing no drug was then restarted to assess the reversibility of drug effects.

### Wireless Cardiac Telemetry Experiments

Male Hartley guinea pigs (Charles River Laboratories) weighing 350–450 g ( $n = 7$  animals) were surgically implanted with wireless cardiac telemetry radio transmitters (model TAICTA-F40; Data Sciences International (DSI), St. Paul, Minnesota). Aseptic surgery was performed to implant a telemeter in the peritoneal cavity of each animal following the general procedures recommended by the manufacturer (DSI). Animals were anesthetized by isoflurane inhalation (4 L/min of isoflurane 3% to induce anesthesia and 1 L/min to maintain it). A midline abdominal incision was made in the skin and muscle layers. The body of the telemeter was laid gently onto the intestines and attached to the overlying muscle wall with non-absorbable sutures. The muscle wall was then closed with absorbable sutures. The telemeter is equipped with two leads for sensing the heart electrical activity; these leads ran through small punctures made in the muscle wall to exteriorize them from the peritoneal cavity. The final position of the telemeter leads was with the negative lead tip near the right shoulder and the positive lead tip below the left axilla on the fifth left rib; this simulates a conventional lead II electrocardiography (ECG). The abdominal skin was then closed with surgical staples, and the animals were allowed to recover for 2 weeks. Immediately after the surgery, animals were administered ketoprofen 1 mg/kg daily subcutaneously (s.c.) for 3 days to reduce postoperative pain and inflammation. They were also administered a single dose of enrofloxacin (2.5 mg/kg, s.c.) to prevent perioperative infections.

Electrocardiography data were collected continuously using the Dataquest A.R.T. acquisition system (version 4.1) from DSI 15 days after surgery. Continuous recording was started 30 min prior to the i.p. injection of rosuvastatin (10 mg/kg, dissolved in saline 0.9%) and continued up to 24 h after the injection. ECG signals were sampled at 1000 Hz. RR and QT

intervals were analyzed using the Ponemah electrophysiology platform (DSI) using the ECG module. QT was corrected by using the Van de Water formula [ $QT_{c,w} = QT - 0.087 \times (RR - 1000)$ ], which has been shown to be more “conservative” for correcting the QT interval in conscious guinea pigs and dogs than the Bazett or the Fridericia formulas, both of which tend to overcorrect the QT at rapid heart rates.<sup>32,33</sup>

### Statistical Analyses

All values are expressed as mean  $\pm$  SEM. Student's paired *t*-test was performed on the magnitude of rosuvastatin's effects on the MAP duration at 90% repolarization (MAPD<sub>90</sub>) at BCLs of 250, 200, and 150 ms using statistical tools in SigmaPlot (Jandel Scientific Software, San Rafael, California). Differences were considered significant at a *p* value less than 0.05. Student's unpaired *t*-test was performed to assess the rate dependency of rosuvastatin's effects on MAPD<sub>90</sub> for BCL250 versus BCL200 and BCL200 versus BCL150. Differences were considered significant at a *p* value less than 0.05. Student's paired *t*-test was performed on the magnitude of rosuvastatin's effects on the prolongation of QT<sub>c,w</sub>.

## RESULTS

### Patch Clamp Experiments and IC<sub>50</sub> Curve Determination

Patch clamp experiments were conducted in hERG-stably transfected HEK 293 cells in order to test the effects of rosuvastatin on the hERG tail current amplitudes. Figure 2 (upper panel) shows the currents elicited in a hERG-stably transfected HEK 293 cell perfused under control conditions (baseline) after exposition to rosuvastatin 78.4 nM and after a 20 min washout period. In this cell, rosuvastatin caused a 25% reduction of the tail current amplitude elicited by a 0 mV activating pulse. Concentrations of 19.6, 78.4, 156.8, 313.6, and 979.2 nM of rosuvastatin were tested. For each of these concentrations and after an activating pulse of +50 mV, tail currents of hERG relative to the baseline were (mean  $\pm$  SEM) 0.872  $\pm$  0.013 (*n* = 7), 0.756  $\pm$  0.043 (*n* = 6), 0.577  $\pm$  0.075 (*n* = 5), 0.435  $\pm$  0.018 (*n* = 8), and 0.277  $\pm$  0.034 (*n* = 5), respectively. These data were fitted to Hill's equation, which gave an estimated IC<sub>50</sub> of 195 nM [95% confidence interval (CI): 62–612] (Fig. 2, lower panel), with a fitted maximum inhibition of 71.6%, Hill's coefficient of -1.92, and *r*<sup>2</sup> of 0.9986.

### Effects of Transporters on hERG Block by Rosuvastatin

Patch clamp experiments were performed on HEK 293-hERG cells exposed to 156.8 nM rosuvastatin and coexpressing different efflux or influx transporters (Fig. 3). Concentration of rosuvastatin was

fixed slightly below the predefined IC<sub>50</sub> (195 nM) to avoid maximal block of hERG under various conditions tested. First, we did a coexpression of hERG with the efflux transporter BCRP. Although the block of hERG current was still observable in the presence of this transporter, it was strongly reduced as compared with the extent of block obtained in HEK 293-hERG cells without transporters [ $17 \pm 4\%$  (*n* = 6) vs.  $42 \pm 8\%$  (*n* = 5); *p* < 0.05]. We propose that this is mostly due to a decrease in the amount of drug in the intracellular compartment. Then, we performed site-directed mutagenesis on BCRP and produced three variants associated with a loss of function of the protein: C421A (Q141K), T623C (F208S), and G1322A (S441N).<sup>34–36</sup> The coexpression of hERG with one or the other of these variants blunted the effects observed with the native efflux transporter BCRP, that is, the block was in the order of 40%. Indeed, inhibition of hERG was  $40 \pm 4$  (*n* = 5),  $41 \pm 7$  (*n* = 7), and  $41 \pm 4$  (*n* = 7) for Q141K, F208S, and S441N, respectively (all not different from control, but different from HEK 293-hERG cells with functional transporters; *p* < 0.05). We also conducted experiments while coexpressing the efflux transporter MDR1 in the hERG-stably expressed HEK 293 cell line. Rosuvastatin is a weak substrate of MDR1, and the block of hERG by rosuvastatin [ $27 \pm 6\%$  (*n* = 6, *p* < 0.05)] in these cells was less than that in the control cells, but more than in those coexpressing the efflux transporter BCRP.<sup>37</sup> Finally, we did an experiment with the influx transporter OATP2B1, which is found in the heart and for which rosuvastatin shows affinity.<sup>38,39</sup> As expected (an influx transporter increases the intracellular concentrations of drugs), we tended to observe an increase in the block of hERG induced by rosuvastatin as compared with the control cells [ $48 \pm 3$  (*n* = 6) vs.  $42 \pm 8$  (*n* = 5); *p* = NS].

### Langendorff Retroperfusion Experiments

Figure 4 shows the typical recordings of ventricular epicardial MAPs of Langendorff retroperfused, isolated guinea pig hearts (*n* = 11) at the baseline (solid tracing) and after a 20-min exposure to rosuvastatin 195 nM (dashed tracing). The effects of the drug on MAPD<sub>90</sub> at BCLs of 150, 200, and 250 ms are shown in Table 1. Rosuvastatin 195 nM caused a typical reverse-rate-dependent prolongation of MAPD<sub>90</sub> associated with I<sub>Kr</sub>-blocking drugs. Indeed, the drug prolonged MAPD<sub>90</sub> by  $4 \pm 1$ ,  $7 \pm 1$ , and  $11 \pm 1$  ms at BCLs of 150, 200, and 250 ms, respectively (*p* < 0.001 vs. baseline at BCL 200; *p* < 0.001 vs. baseline at BCL 250; *p* < 0.01 vs. baseline at BCL 150). Moreover, increase in MAPD<sub>90</sub> was more important at BCL250 versus BCL200 ( $+11 \pm 1$  vs.  $+7 \pm 1$  ms; *p* < 0.01) and more important at BCL200 versus BCL150 ( $+7 \pm 1$  vs.  $+4 \pm 1$  ms; *p* < 0.05).

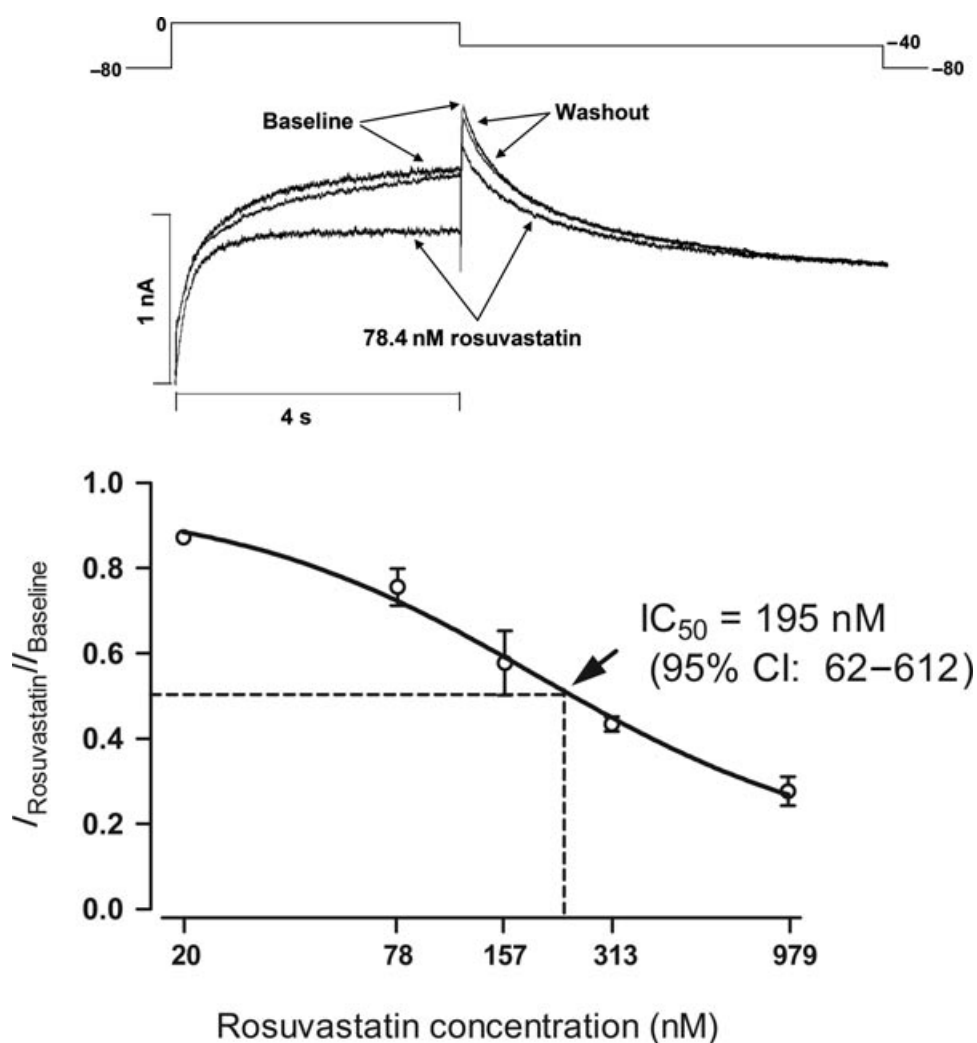


**Figure 2.** Activating and tail currents elicited, respectively, by a 4-s step to 0 mV and a 6-s step to -40 mV in a hERG-stably transfected HEK 293 cell. Currents elicited are shown under control conditions (baseline), after 15 min of perfusion with 78.4 nM rosuvastatin, and after 20 min of washout (upper panel). The lower panel illustrates the hERG tail current amplitudes normalized to control ( $n = 31$  cells) plotted as a function of rosuvastatin concentration and fitted to the Hill's equation.

### Wireless Cardiac Telemetry Experiments

Upper panel of Figure 5 shows the typical recordings of lead II ECG in conscious and unrestrained guinea pigs before and after a single i.p. injection of rosuvastatin (10 mg/kg). In this animal, rosuvastatin caused a 9-ms prolongation of the QT interval. When QT is corrected for the heart rate using the Van de Water formula [ $QT_{cVW} = QT - 0.087 \times (RR - 1000)$ ],  $QT_{cVW}$  goes from 201 ms at the baseline to 210 ms 120–150 min after a single i.p. injection of rosuvastatin (10 mg/kg). Lower panel of Figure 5 shows the individual effect of rosuvastatin (10 mg/kg, i.p.) on  $QT_{cVW}$  in conscious and unrestrained guinea pigs ( $n = 7$ ) implanted with cardiac telemetry radio transmitters. On average ( $n = 7$ ),  $QT_{cVW}$  was prolonged from  $201 \pm 1$  ms at the baseline to  $210 \pm 2$  ms approximately 120–150 min af-

ter a single i.p. injection of rosuvastatin (10 mg/kg), giving an average prolongation of  $9 \pm 1$  ms of  $QT_{cVW}$  ( $p < 0.001$  vs. baseline). At the 120-min time point, preliminary studies in animals injected with rosuvastatin (10 mg/kg, i.p.) showed that plasma levels of the drug vary between 189 and 628 nM. Saline-injected animals ( $n = 4$ ) showed a  $-2.0 \pm 0.9$  ms variation ( $p = NS$ ) in the QT interval.

### DISCUSSION

Results obtained in this study demonstrate that rosuvastatin blocks the hERG current with an  $IC_{50}$  of 195 nM. Rosuvastatin also prolongs  $MAPD_{90}$  by 10 ms in isolated guinea pig hearts (195 nM) and prolongs the QT interval in animals injected with

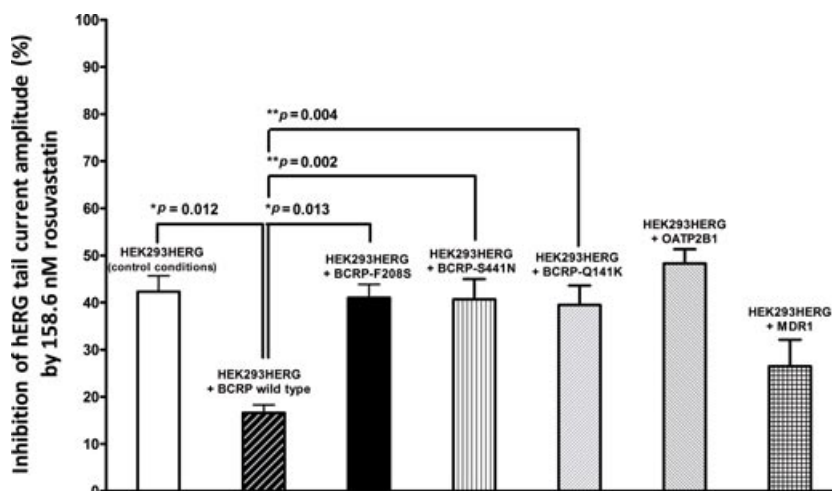


**Figure 3.** Percent inhibition of hERG tail current amplitude by rosuvastatin (156.8 nM) in HEK 293 hERG cells and in cells coexpressing various efflux (BCRP or MDR1) or influx (OATP2B1) transporters. Inhibition of current activity was also determined in cells expressing transporters with a loss of function in BCRP activity due to mutations (BCRP-F208S, BCRP-S441N, and BCRP-Q141K).

the drug (10 mg/kg). A concentration of 195 nM can be easily achieved and exceeded at peak plasma concentrations of the drug in patients with decreased clearance due to genetic polymorphisms or drug–drug interactions.<sup>27–31</sup> We have demonstrated that the block of hERG by rosuvastatin is modulated by influx and efflux drug transporters involved in the disposition and cardiac distribution of the drug. These results lead us to propose that some patients with

genetic defects or receiving concomitant drug therapies may be at risk of rosuvastatin-induced long QT syndrome (LQTS) due to significant block of  $I_{Kr}$  and increased cardiac intracellular concentrations of the drug.

Rosuvastatin shows many advantages as compared with other statins, such as low extrahepatic cellular penetration, low potential for CYP3A4 drug interactions, capacity to produce a substantial high-density

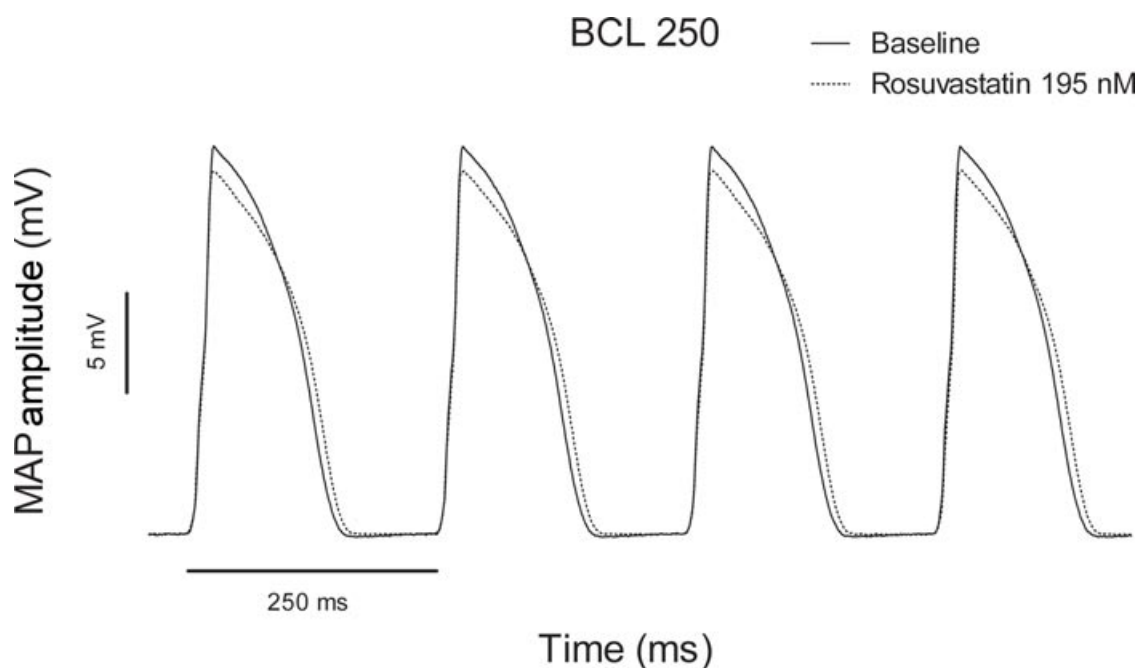


**Figure 4.** Typical recordings of ventricular epicardial monophasic action potentials from Langendorff retroperfused, isolated guinea pig hearts paced at a BCL of 250 ms at baseline (solid tracing) and after a 20-min exposure to rosuvastatin 195 nM (dashed tracing).

**Table 1.** Effects of Rosuvastatin 195 nM on MAPD<sub>90</sub> at BCLs of 150, 200, and 250 ms

BCL (ms)	Baseline MAPD <sub>90</sub> (ms)	Rosuvastatin 195 nM MAPD <sub>90</sub> (ms)	Changes in MAPD <sub>90</sub> (ms)
150	106 ± 3	110 ± 3***	+4 ± 1
200	125 ± 3	132 ± 4***	+7 ± 1*
250	138 ± 4	149 ± 4***	+11 ± 1**

\*\*\* $p < 0.001$  versus baseline, \*\* $p < 0.01$  versus variation of MAPD<sub>90</sub> at BCL 200, \* $p < 0.05$  versus variation of MAPD<sub>90</sub> at BCL 150.

lipoprotein cholesterol increase, and a reduction of LDL cholesterol to a greater extent than atorvastatin, simvastatin, and pravastatin.<sup>40</sup> Compared with atorvastatin, simvastatin, cerivastatin, fluvastatin, and pravastatin, rosuvastatin is a more potent inhibitor of hepatocyte sterol synthesis.<sup>40</sup> Rosuvastatin is available as oral tablets of 5, 10, 20, and 40 mg (CRESTOR product monograph). At steady state, a dosing of 40 mg produces, on average, a  $C_{max}$  of about 20 ng/mL (39.2 nM). However, there is a large inter-subject variability, and the peak plasma levels can vary from 10 to 100 ng/mL (21–208 nM).<sup>27</sup>

The presence of a stable polar methanesulfonamide group in the rosuvastatin structure confers an en-

hanced interaction with the HMG-CoA enzyme.<sup>41,42</sup> Unfortunately, this moiety also generally confers a high affinity for the hERG potassium channel. To date, no clinical case of ventricular arrhythmias and torsades de pointes have been reported in patients treated with rosuvastatin. Our data should then still be considered as theoretical. However, drug-induced torsades de pointes is a very rare event, even for well-characterized QT-prolonging drugs such as cisapride, terfenadine, pimozone, droperidol, domperidone, and so on. For instance, it is believed that drug-induced torsades de pointes are observed in 1:100,000 patients with these drugs. In 2002, Barbey et al.<sup>43</sup> could identify only 391 cases of torsades de pointes with cisapride, even though, in the 1990s, the drug was used daily by millions of individuals. The use of rosuvastatin remains limited as compared with other QT-prolonging drugs both for time of exposure and number of patients taking the drug. The largest clinical trial with rosuvastatin is the Jupiter study, with 5000 patients.

Finally, well-designed mechanistic studies are often the best way to identify drugs associated with LQTS. For instance, in the case of cisapride, Walker et al.<sup>44</sup> reviewed the use of cisapride in 36,743

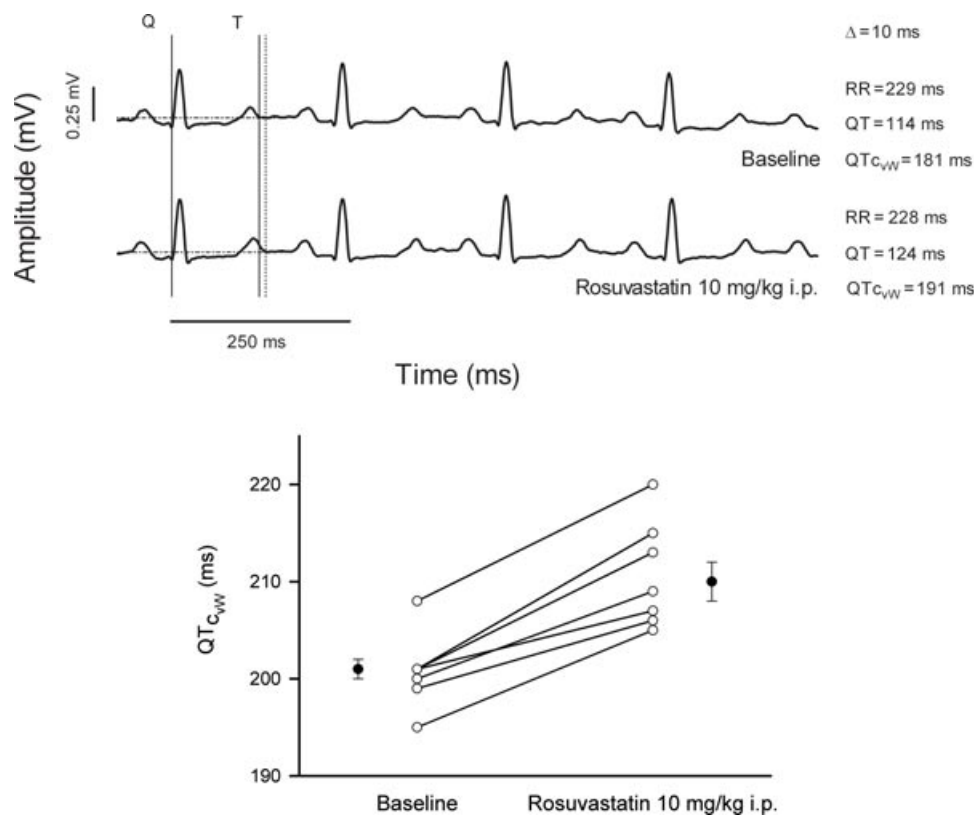


**Figure 5.** Upper panel shows the typical lead II guinea pig ECG tracings recorded at baseline and 120–150 min after a single i.p. injection of rosuvastatin (10 mg/kg). Vertical lines indicate where cursors were placed for QT interval measurements. Lower panel shows the individual effects of rosuvastatin (10 mg/kg, i.p.) on QT<sub>cVW</sub> in conscious and unrestrained guinea pigs ( $n = 7$ ) implanted with cardiac telemetry radio transmitters.



patients and could not find any link between cisapride use and LQTS; the odds ratio for cisapride use and cardiac outcomes was 1 (95% CI 0.3–3.7). However, at the same time, mechanistic *in vitro* (patch clamp) studies, *ex vivo* studies (explanted hearts), *in vivo* animal models, and case reports in patients were all pointing toward the conclusion that cisapride use is associated with an increased risk of drug-induced LQTS and death in certain patients.<sup>15</sup>

Hepatic uptake of rosuvastatin involves transporters such as OATP1B1, OATP1B3, and OATP2B1.<sup>26</sup> Following oral administration, the drug is predominantly secreted from the hepatocytes to the canalicular bile tract by the efflux transporter BCRP such that approximately 72% of absorbed rosuvastatin is eliminated via bile secretion and 28% via renal excretion.<sup>28,45</sup> We tested the effects of rosuvastatin on hERG tail current in cells coexpressing efflux transporters such as BCRP and MDR1 or the influx transporter OATP2B1. BCRP and MDR1 are strong and weak efflux transporters, respectively, of rosuvastatin.<sup>37</sup> These transporters were selected because their expression in human cardiac tissue had been previously demonstrated.<sup>46</sup> We observed a large decrease in the percentage of block of hERG in the presence of BCRP as compared with the control cells ( $17 \pm 4\%$  vs.  $42 \pm 8\%$ ), this decrease being more discrete in the presence of MDR1 ( $27 \pm 6\%$  vs.  $42 \pm 8\%$ ). When the hERG current was coexpressed with the influx transporter OATP2B1, the percentage of block tended to increase from  $42 \pm 8\%$  to  $48 \pm 3\%$ . These results suggest that these transporters control the access of the drug to well-characterized intracellular binding sites to hERG and consequently, extent of channel block by rosuvastatin.

We also tested the effects of rosuvastatin on hERG in the presence of three loss-of-function polymorphisms of BCRP (Q141K, F208S, and S441N) and observed a block comparable to the one found in the control cells ( $\approx 42\%$ ). These polymorphisms are found in humans with relatively high frequencies (0.3%–25%), especially for Q141K (25% of Caucasians).<sup>47</sup> Patients sharing a loss of function in BCRP (*ABCG2* 421AA; 1.2%) and OATP1B1 (*SLCO1B1* 521CC; 2%), the major efflux transporters involved in the disposition of rosuvastatin, or a gain of function polymorphism in OATP2B1 (*SLCO2B1* 935GG; 10%) should use rosuvastatin with caution due to increased plasma and cardiac levels. Hence, under normal conditions, membrane transporters appear protective of rosuvastatin's effects on  $I_{Kr}$ . Genetic polymorphisms or block of the transporters (gemfibrozil, lopinavir/ritonavir, cyclosporine) may increase the likelihood of potentially deleterious effects of rosuvastatin on  $I_{Kr}$ .<sup>28–30</sup>

## CONCLUSION

We demonstrated that rosuvastatin blocks the hERG current and causes prolongation of MAPD<sub>90</sub> and QT intervals in well-established electrophysiological models. Blunting of rosuvastatin-induced block of hERG following the coexpression of the efflux membrane transporter BCRP provides a rationale for the low frequency of rosuvastatin-induced LQTS. Our results suggest that a subpopulation of patients with a decreased clearance of the drug due to genetic polymorphisms or inhibition of BCRP/OATP1B1 due to concomitant drugs might be at an increased risk of drug-induced proarrhythmic effects.

## ACKNOWLEDGMENTS

This work was supported by the Fondation des maladies du coeur du Québec (18497, to Jacques Turgeon), the Fonds d'Enseignement et de Recherche de la Faculté de pharmacie de l'Université Laval (Master Studentship Award to Patrick Vigneault), and the Fonds de la recherche en santé du Québec (Scholarship Award to Benoît Drolet). We thank François Bélanger for his collaboration in experiments related with the expression of membrane transporters. We also thank Sylvie Pilote for her collaboration in the Langendorff and telemetry experiments.

## REFERENCES

- Li GR, Feng J, Yue L, Carrier M, Nattel S. 1996. Evidence for two components of delayed rectifier K<sup>+</sup> current in human ventricular myocytes. *Circ Res* 78(4):689–696.
- Sanguinetti MC, Jiang C, Curran ME, Keating MT. 1995. A mechanistic link between an inherited and an acquired cardiac arrhythmia: HERG encodes the  $I_{Kr}$  potassium channel. *Cell* 81(2):299–307.
- Sanguinetti MC, Curran ME, Zou A, Shen J, Spector PS, Atkinson DL, Keating MT. 1996. Coassembly of K<sub>v</sub>LQT1 and minK (IsK) proteins to form cardiac  $I_{Ks}$  potassium channel. *Nature* 384(6604):80–83.
- Sanguinetti MC, Jurkiewicz NK. 1990. Two components of cardiac delayed rectifier K<sup>+</sup> current. Differential sensitivity to block by class III antiarrhythmic agents. *J Gen Physiol* 96(1):195–215.
- Carmeliet E. 1992. Voltage- and time-dependent block of the delayed K<sup>+</sup> current in cardiac myocytes by dofetilide. *J Pharmacol Exp Ther* 262(2):809–817.
- Krafte DS, Volberg WA. 1994. Voltage dependence of cardiac delayed rectifier block by methanesulfonamide class III antiarrhythmic agents. *J Cardiovasc Pharmacol* 23(1):37–41.
- Yang T, Snyders DJ, Roden DM. 1995. Ibutilide, a methanesulfonanilide antiarrhythmic, is a potent blocker of the rapidly activating delayed rectifier K<sup>+</sup> current ( $I_{Kr}$ ) in AT-1 cells. Concentration-, time-, voltage-, and use-dependent effects. *Circulation* 91(6):1799–1806.
- Arena JP, Kass RS. 1988. Block of heart channels by clofilium and its tertiary analogs: Relationship between drug structure and type of channel blocked. *Mol Pharmacol* 34(1):60–66.

9. Turgeon J, Daleau P, Bennett PB, Wiggins SS, Selby L, Roden DM. 1994. Block of  $I_{Ks}$ , the slow component of the delayed rectifier  $K^+$  current, by the diuretic agent indapamide in guinea pig ventricular myocytes. *Circ Res* 75(5):879–886.
10. Heath BM, Terrar DA. 1996. Separation of the components of the delayed rectifier potassium current using selective blockers of  $I_{Kr}$  and  $I_{Ks}$  in guinea-pig isolated ventricular myocytes. *Exp Physiol* 81(4):587–603.
11. Ekins S. 2004. Predicting undesirable drug interactions with promiscuous proteins *in silico*. *Drug Discov Today* 9(6):276–285.
12. Brown AM. 2004. Drugs, hERG and sudden death. *Cell Calcium* 35(6):543–547.
13. Pearlstein R, Vaz R, Rampe D. 2003. Understanding the structure–activity relationship of the human ether-a-go-go-related gene cardiac  $K^+$  channel. A model for bad behavior. *J Med Chem* 46(11):2017–2022.
14. Drici MD, Barhanin J. 2000. Cardiac  $K^+$  channels and drug-acquired long QT syndrome. *Therapie* 55(1):185–193.
15. Drolet B, Khalifa M, Daleau P, Hamelin BA, Turgeon J. 1998. Block of the rapid component of the delayed rectifier potassium current by the prokinetic agent cisapride underlies drug-related lengthening of the QT interval. *Circulation* 97(2):204–210.
16. Drolet B, Rousseau G, Daleau P, Cardinal R, Turgeon J. 2000. Domperidone should not be considered a no-risk alternative to cisapride in the treatment of gastrointestinal motility disorders. *Circulation* 102(16):1883–1885.
17. Drolet B, Yang T, Daleau P, Roden DM, Turgeon J. 2003. Risperidone prolongs cardiac repolarization by blocking the rapid component of the delayed rectifier potassium current. *J Cardiovasc Pharmacol* 41(6):934–937.
18. Daleau P, Lessard E, Groleau MF, Turgeon J. 1995. Erythromycin blocks the rapid component of the delayed rectifier potassium current and lengthens repolarization of guinea pig ventricular myocytes. *Circulation* 91(12):3010–3016.
19. Drolet B, Vincent F, Rail J, Chahine M, Deschênes D, Nadeau S, Khalifa M, Hamelin BA, Turgeon J. 1999. Thioridazine lengthens repolarization of cardiac ventricular myocytes by blocking the delayed rectifier potassium current. *J Pharmacol Exp Ther* 288(3):1261–1268.
20. Drolet B, Zhang S, Deschênes D, Rail J, Nadeau S, Zhou Z, January CT, Turgeon J. 1999. Droperidol lengthens cardiac repolarization due to block of the rapid component of the delayed rectifier potassium current. *J Cardiovasc Electrophysiol* 10(12):1597–1604.
21. Khalifa M, Drolet B, Daleau P, Lefez C, Gilbert M, Plante S, O'Hara GE, Gleeton O, Hamelin BA, Turgeon J. Block of potassium currents in guinea pig ventricular myocytes and lengthening of cardiac repolarization in man by the histamine H1 receptor antagonist diphenhydramine. *J Pharmacol Exp Ther* 288(2):858–865.
22. Geelen P, Drolet B, Rail J, Bérubé J, Daleau P, Rousseau G, Cardinal R, O'Hara GE, Turgeon J. 2000. Sildenafil (Viagra) prolongs cardiac repolarization by blocking the rapid component of the delayed rectifier potassium current. *Circulation* 102(3):275–277.
23. Drolet B, Rousseau G, Daleau P, Cardinal R, Simard C, Turgeon J. 2001. Pimozide (Orap) prolongs cardiac repolarization by blocking the rapid component of the delayed rectifier potassium current in native cardiac myocytes. *J Cardiovasc Pharmacol Ther* 6(3):255–260.
24. Ridker PM, Danielson E, Fonseca FA, Genest J, Gotto AM Jr, Kastelein JJ, Koenig W, Libby P, Lorenzatti AJ, MacFadyen JG, Nordestgaard BG, Shepherd J, Willerson JT, Glynn RJ, JUPITER Study Group. 2008. Rosuvastatin to prevent vascular events in men and women with elevated C-reactive protein. *N Engl J Med* 359(21):2195–2207.
25. Martin PD, Warwick MJ, Dane AL, Hill SJ, Giles PB, Philips PJ, Lenz E. 2003. Metabolism, excretion, and pharmacokinetics of rosuvastatin in healthy adult male volunteers. *Clin Ther* 25(11):2822–2835.
26. Ho RH, Tirona RG, Leake BF, Glaeser H, Lee W, Lemke CJ, Wang Y, Kim RB. 2006. Drug and bile acid transporters in rosuvastatin hepatic uptake: Function, expression, and pharmacogenetics. *Gastroenterology* 130(6):1793–1806.
27. Lee E, Ryan S, Birmingham B, Zalickowski J, March R, Ambrose H, Moore R, Lee C, Chen Y, Schneck D. 2005. Rosuvastatin pharmacokinetics and pharmacogenetics in white and Asian subjects residing in the same environment. *Clin Pharmacol Ther* 78(4):330–341.
28. Simonson SG, Raza A, Martin PD, Mitchell PD, Jarcho JA, Brown CD, Windass AS, Schneck D. 2004. Rosuvastatin pharmacokinetics in heart transplant recipients administered an antirejection regimen including cyclosporine. *Clin Pharmacol Ther* 76(2):167–177.
29. Kiser JJ, Gerber JG, Predhomme JA, Wolfe P, Flynn DM, Hoody DW. 2008. Drug/drug interaction between lopinavir/ritonavir and rosuvastatin in healthy volunteers. *J Acquir Immune Defic Syndr* 47(5):570–578.
30. Bergman E, Matsson EM, Hedeland M, Bondesson U, Knutson L, Lennernas H. 2010. Effect of a single gemfibrozil dose on the pharmacokinetics of rosuvastatin in bile and plasma in healthy volunteers. *J Clin Pharmacol* 50:1039–1049.
31. Keskitalo JE, Zolk O, Fromm MF, Kurkinen KJ, Neuvonen PJ, Niemi M. 2009. ABCG2 polymorphism markedly affects the pharmacokinetics of atorvastatin and rosuvastatin. *Clin Pharmacol Ther* 86(2):197–203.
32. Sakaguchi Y, Takahara A, Nakamura Y, Akie Y, Sugiyama A. 2009. Halothane-anaesthetized, closed-chest, guinea-pig model for assessment of drug-induced QT-interval prolongation. *Basic Clin Pharmacol Toxicol* 104(1):43–48.
33. De Clerck F, Van de WA, D'Aubioul J, Lu HR, van Rossem K, Hermans A, Van Ammel K. 2002. *In vivo* measurement of QT prolongation, dispersion and arrhythmogenesis: Application to the preclinical cardiovascular safety pharmacology of a new chemical entity. *Fundam Clin Pharmacol* 16(2):125–140.
34. Kondo C, Suzuki H, Itoda M, Ozawa S, Sawada J, Kobayashi D, Ieiri I, Mine K, Ohtsubo K, Sugiyama Y. 2004. Functional analysis of SNPs variants of BCRP/ABCG2. *Pharm Res* 21(10):1895–1903.
35. Tamura A, Wakabayashi K, Onishi Y, Takeda M, Ikegami Y, Sawada S, Tsuji M, Matsuda Y, Ishikawa T. 2007. Re-evaluation and functional classification of non-synonymous single nucleotide polymorphisms of the human ATP-binding cassette transporter ABCG2. *Cancer Sci* 98(2):231–239.
36. Yoshioka S, Katayama K, Okawa C, Takahashi S, Tsukahara S, Mitsuhashi J, Sugimoto Y. 2007. The identification of two germ-line mutations in the human breast cancer resistance protein gene that result in the expression of a low/non-functional protein. *Pharm Res* 24(6):1108–1117.
37. Huang L, Wang Y, Grimm S. 2006. ATP-dependent transport of rosuvastatin in membrane vesicles expressing breast cancer resistance protein. *Drug Metab Dispos* 34(5):738–742.
38. Grube M, Köck K, Oswald S, Draber K, Meissner K, Eckel L, Böhm M, Felix SB, Vogelgesang S, Jedlitschky G, Siegmund W, Warzok R, Kroemer HK. 2006. Organic anion transporting polypeptide 2B1 is a high-affinity transporter for atorvastatin and is expressed in the human heart. *Clin Pharmacol Ther* 80(6):607–620.
39. Kitamura S, Maeda K, Wang Y, Sugiyama Y. 2008. Involvement of multiple transporters in the hepatobiliary transport of rosuvastatin. *Drug Metab Dispos* 36(10):2014–2023.
40. McTaggart F. 2003. Comparative pharmacology of rosuvastatin. *Atheroscler Suppl* 4(1):9–14.

41. Watanabe M, Koike H, Ishiba T, Okada T, Seo S, Hirai K. 1997. Synthesis and biological activity of methanesulfonamide pyrimidine- and N-methanesulfonyl pyrrole-substituted 3,5-dihydroxy-6-heptenoates, a novel series of HMG-CoA reductase inhibitors. *Bioorg Med Chem* 5(2):437-444.
42. Istvan ES, Deisenhofer J. 2001. Structural mechanism for statin inhibition of HMG-CoA reductase. *Science* 292(5519):1160-1164.
43. Barbey JT, Lazzara R, Zipes DP. 2002. Spontaneous adverse event reports of serious ventricular arrhythmias, QT prolongation, syncope, and sudden death in patients treated with cisapride. *J Cardiovasc Pharmacol Ther* 7(2):65-76.
44. Walker AM, Szneke P, Weatherby LB, Dicker LW, Lanza LL, Loughlin JE, Yee CL, Dreyer NA. 1999. The risk of serious cardiac arrhythmias among cisapride users in the United Kingdom and Canada. *Am J Med* 107(4):356-362.
45. McTaggart F, Buckett L, Davidson R, Holdgate G, McCormick A, Schneck D, Smith G, Warwick M. 2001. Preclinical and clinical pharmacology of rosuvastatin, a new 3-hydroxy-3-methylglutaryl coenzyme A reductase inhibitor. *Am J Cardiol* 87(5A):28B-32B.
46. Couture L, Nash JA, Turgeon J. 2006. The ATP-binding cassette (ABC) transporters and their implication in drug disposition: A special look at the heart. *Pharmacol Rev* 58(2):244-258.
47. Zamber CP, Lamba JK, Yasuda K, Farnum J, Thummel K, Schuetz JD, Schuetz EG. 2003. Natural allelic variants of breast cancer resistance protein (BCRP) and their relationship to BCRP expression in human intestine. *Pharmacogenetics* 13(1):19-28.